

# Self-assembly in inorganic and hybrid systems: beyond the molecular scale

Markus Antonietti,<sup>\*a</sup> Markus Niederberger<sup>b</sup> and Bernd Smarsly<sup>a</sup>

Received 27th July 2007, Accepted 6th September 2007

First published as an Advance Article on the web 17th September 2007

DOI: 10.1039/b711529f

The availability of well defined inorganic nanocrystals allows the construction of aligned structures with characteristic architectural elements in the nanometer range, the mesoscale. Contrary to alignment driven by external conditions and fields, we focus on strict “self-effects”, where the organization is already encoded in the shape and mutual interaction potentials of the particles. This Perspective discusses the potential of this approach for generating valuable functional inorganic mesostructures.

## Introduction

In the development of the chemical sciences, order was presumably first observed in inorganic systems. The beauty of crystals has brought humankind to think in terms of symmetry, but of substances and molecules. Later, the coordination chemistry of Werner taught us about the importance of secondary bonding in structure set-up, and that functionality, along with long range order, can also be created between organic and inorganic components. This finally gave birth to metalorganic supramolecular chemistry in its many variations.<sup>1</sup>

Currently, we are experiencing an extension of these principles towards larger, but also hierarchical structures with more complexity. Through multi-binding and multi-valency, complexes can be turned into coordination polymers,<sup>2</sup> and the expansion of the metal center towards well-defined clusters enabled the set-up of metal-organic frameworks.<sup>3,4</sup> The rules of supramolecular chemistry which govern and enable this complex structure formation are important for this article. For instance, secondary, reversible binding motifs allow reversibility, self-healing and a dynamic-combinatorial self-optimization of the structure.<sup>5</sup> Another typical motif is the formation of structural hierarchies, where every level of integration is activated or encoded in another type of binding: *e.g.* cluster crystallization can be followed by ligand interaction, then by coulombic forces or hydrophobic optimization.<sup>5</sup> The whole structural program is usually already encoded in the primary components and their mixing ratio.

Here, we want to discuss complexity of structure beyond the previous scale, which was revealed simultaneously with the availability of very small solvent-, ligand- or polymer-stabilized crystalline nanoparticles. Due to their small size and the corresponding thermal mobility as well as the inherent tensorial interaction fields found in the crystal symmetry and architecture, these nanoparticles are able to exhibit a series of novel mesoscale self-assembly phenomena:

- The alignment of nanoparticles towards one and two dimensional “polymers” or arrays driven by special ligands or solvent molecules (“assembler”).

- The spontaneous textural alignment of nanoparticles towards oriented monodomains along interfaces, “soft epitaxy”.

- The formation of free, self supporting three dimensional superstructures formed by strongly interacting nanocrystals, which can include organic material, porosity, splay and curvature (“mesocrystals”).

The common features of these structures are discussed, and the special potential of inorganic building blocks for structure set-up and functionality is highlighted.

## Non-aqueous sol-gel chemistry of oxide nanoparticles and their alignment

The preparation of well-defined oxidic nanobuilding blocks in the size range of just a few nanometers, yet with high crystallinity, poses great demands on the control of the reaction parameters at any stage of the synthesis pathway. In our opinion, only soft-chemistry routes and in particular sol-gel procedures are able to meet these strict requirements. The slow transformation of the precursor molecules into the final inorganic structure allows the structural and morphological characteristics of the final products to be influenced by chemical means. Although aqueous processes are still the most common, the notorious complexity of the chemistry of water and its solvent properties necessitates a search for alternative synthetic approaches that allow better control over kinetic as well as thermodynamic parameters. In this respect, non-aqueous sol-gel processes in organic solvents represent a powerful tool for the design of such small nanocrystalline building units. The advantages are closely related to the manifold role of the organic components in the reaction mixture, not only acting as oxygen supplying agents, but also influencing particle size, shape and surface properties.<sup>6</sup> Metal oxide precursors suitable for non-aqueous sol-gel processes range from metal halides, acetates, acetylacetonates, to alkoxides, and also include mixtures thereof for multi-metal oxides. Potential solvents are typically, although not exclusively, oxygen-containing liquids such as alcohols, ketones, or aldehydes. A large and steadily growing number of precursor-solvent combinations give access to metal oxide nanoparticles with a broad range of compositions and a great diversity of particle sizes and shapes.<sup>6,7</sup>

Non-aqueous sol-gel processes are typically performed in a temperature range of 50 to 200 °C. These moderate conditions are a prerequisite in order for the organic species in the reaction

<sup>a</sup>Department of Colloid Chemistry, Max Planck Institute of Colloids and Interfaces, Research Campus Golm, D-14424, Potsdam, Germany. E-mail: pape@mpikg-golm.mpg.de; Fax: +49 331 567 9502

<sup>b</sup>Department of Materials, ETH Zürich, Wolfgang-Pauli-Strasse 10, CH-8093 Zürich, Switzerland



**Markus Antonietti**

*Markus Antonietti's contributions to the chemical community comprise manifold things, but most of all he is interested in creativity in research. He loves to share and impart this passion. He likes cooking with his family and loud music.*

*Markus Antonietti has studied chemistry in Mainz and carried out his doctorate with Hans Sillescu. His habilitation about nanostructured polymeric gels in 1990 filled him with enthusiasm for complex materials. After his professorship in chemistry at the University of Marburg he was appointed Director of the Department of Colloid Chemistry at the Max Planck Institute of Colloids and Interfaces in 1993.*



**Markus Niederberger**

*Markus Niederberger studied chemistry at the Swiss Federal Institute of Technology (ETH) Zürich, where he also received his PhD degree in 2000. After a postdoctoral stay at the University of California at Santa Barbara, he became group leader at the Max Planck Institute of Colloids and Interfaces at Potsdam in 2002. Since 2007 he is Assistant Professor in the Department of Materials at ETH Zürich. His primary research interests are the development of general synthetic concepts for inorganic nanoparticles, investigation of formation and crystallization mechanisms and nanoparticle assembly.*

*Markus Niederberger studied chemistry at the Swiss Federal Institute of Technology (ETH) Zürich, where he also received his PhD degree in 2000. After a postdoctoral stay at the University of California at Santa Barbara, he became group leader at the Max Planck Institute of Colloids and Interfaces at Potsdam in 2002. Since 2007 he is Assistant Professor in the Department of Materials at ETH Zürich. His primary research*



**Bernd Smarsly**

*Bernd Smarsly studied chemistry and physics at the University of Marburg, Germany, and Innsbruck, Austria, and received a Master's degree of Natural Science in 1998. He completed his PhD studies in 2001 at the Max Planck Institute of Colloids and Interfaces. After a Postdoctoral fellowship at University of New Mexico in Albuquerque (2002–2003) he stayed at MPI of Colloids and Interfaces until 2007 as group leader. He now works as professor of physical chemistry at the University of Giessen (Germany). His main research interests focus on the preparation of functional, mesostructured metal oxides, their physico-chemical properties and the development of novel characterization techniques, especially using X-ray scattering.*

*Bernd Smarsly studied chemistry and physics at the University of Marburg, Germany, and Innsbruck, Austria, and received a Master's degree of Natural Science in 1998. He completed his PhD studies in 2001 at the Max Planck Institute of Colloids and Interfaces. After a Postdoctoral fellowship at University of New Mexico in Albuquerque (2002–2003) he stayed at MPI of Colloids and Interfaces until 2007 as group leader. He now works*

mixture to fulfil its complex role as reactant and crystal growth modifier. For systems with sufficient anisotropy and interactions, the solvent also acts to support organized assembly of the particles, and dissolution of additional, face selective ligands ("assembler") even refine the textural organization.

The synthesis of tungsten oxide nanoparticles and nanostructures constitutes an illustrative example as to how precursor, solvent and additional ligands influence crystallite size, shape and assembly behaviour. The reaction of tungsten chloride with benzyl alcohol yielded tungsten nanoplatelets with a relatively broad size distribution of 30 to 100 nm (Fig. 1a).<sup>8</sup> Addition of the bioligand deferoxamine mesylate, a siderophore, changes the particle morphology completely from a pseudo-2D shape to 1D nanowire bundles (Fig. 1b). These nanowires are single-crystalline and exhibit a uniform diameter of 1.3 nm (Fig. 1c).<sup>9</sup> If a small amount of 4-*tert*-butylcatechol is added to the tungsten chloride–

benzyl alcohol mixture, anisotropic rod-like architectures with diameters between 35 and 40 nm are observed (Fig. 1d).<sup>10</sup> The rods consist of a highly ordered, lamellar organic–inorganic hybrid nanostructure, where the lamellae are stacked in one direction with high precision. The slightly corrugated sides of the rods are a consequence of the good monodispersity of the nanoparticulate building blocks. No individual or isolated nanoparticles are found in a sample washed in chloroform, whereas many discs and platelets with round corners are detected upon drying and redispersing the brown powder in water (Fig. 1d, inset). This finding clearly gives evidence that the inorganic platelets interact only weakly, *i.e.*, the superstructure is built up by secondary interactions of the organic phase. The reaction between tungsten chloride and 4-*tert*-butylbenzal alcohol (instead of benzyl alcohol) resulted in the formation of a fibrous network. The TEM image reveals ribbon-like structures consisting of parallel columns with

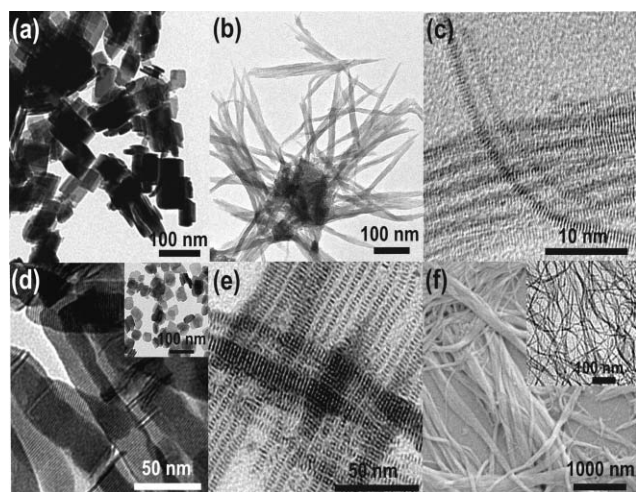


**Fig. 1** TEM or SEM images of various tungsten oxide nanoparticles and nanostructures. a) Nanoplatelets, b) nanowire bundles, c) nanowires (HRTEM image), d) columns of stacked nanoplatelets (inset: separated individual nanoplatelets), e) laterally assembled columns of stacked nanoplatelets, f) nanowire ribbons (inset: separated individual nanowires). Images b)–c) reprinted with permission from J. Polleux, N. Pinna, M. Antonietti and M. Niederberger, *J. Am. Chem. Soc.*, 2005, **127**, 15595–15601.<sup>12</sup> © 2007 American Chemical Society.

uniform diameters of about 4 nm (Fig. 1e).<sup>10</sup> Each nanocolumn is composed of self-aligned nanoplatelets about 1 nm thick and facing each other along the entire length of the nanostack. The individual nanostacks are nearly monodisperse in diameter as a consequence of the uniform-sized platelets, which leads to an outstanding alignment on two levels of hierarchy. It is intriguing to see the tremendous difference in crystal growth and in the assembly of the tungsten oxide building blocks, although 4-*tert*-butylbenzyl alcohol and benzyl alcohol differ only in the presence of a *tert*-butyl group. If the precursor is changed from tungsten chloride to tungsten isopropoxide, tungsten oxide nanowire bundles are obtained in benzyl alcohol without the use of any additional structure-directing templates (Fig. 1f).<sup>11</sup> The nanowires are held together by intercalated benzaldehyde molecules that were formed *in situ* during the synthesis. The bundles can be split up into individual nanowires of 1 nm diameter by the addition of formamide to a dispersion of the nanobundles in ethanol (Fig. 1f, inset). The high surface-to-volume ratio combined with the high purity of the material makes these nanowire bundles ideal candidates for gas-sensing devices. Preliminary results confirm this assumption, as these nanowires show an extraordinarily good sensitivity to NO<sub>2</sub> concentrations in the ppb range.<sup>11</sup>

In fact, the plates forming the extended stacks in Fig. 1d are not single crystals, but superstructures themselves. This is illustrated and explained in Fig. 2.

With respect to the use of nanoparticles as building blocks for the bottom-up fabrication of hierarchically ordered nanostructures, it is of utmost importance that preformed nanoparticles can be arranged and patterned with high precision. An attractive strategy following the arguments above involves the encoding of the assembly behaviour of the nanoparticles by surface functionalization with so-called assembler molecules—small polydentate organic ligands. In order to build up one-, two- and three-dimensional superstructures in a controlled way (all exemplified in the WO<sub>3</sub>-

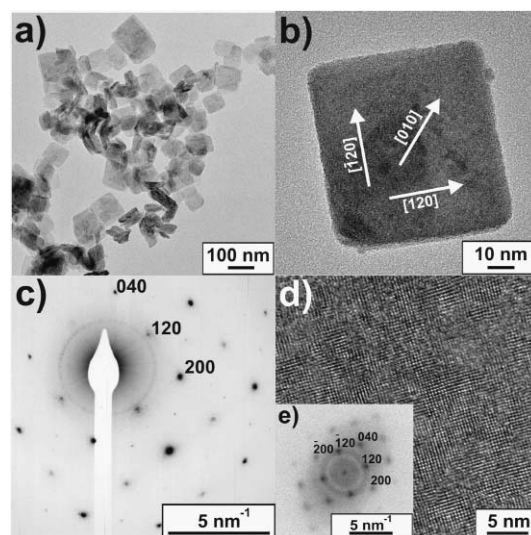


**Fig. 2** More detailed analysis of the “beer mat particles” forming the stacks shown in 1d: a) overview of the non-stacked particles, b) higher magnification of one particle indicating rounded corners; c) corresponding electron diffraction picture indicating apparent single crystal character; d) high magnification of the same particle indicating that the plate is an oriented mosaic pattern of primary particles *ca.* 5 nm in size. Reprinted with permission from J. Polleux, N. Pinna, M. Antonietti and M. Niederberger, *J. Am. Chem. Soc.*, 2005, **127**, 15595–15601.<sup>12</sup> © 2007 American Chemical Society.

case), the nanosized building blocks have to exhibit an anisotropic surface reactivity, and the assembler molecules are able to provide this feature either by selective binding to specific crystal faces, or by selective desorption from specific crystal faces. An instructive example of this was reported for anatase nanoparticles of 5 nm in diameter which were synthesized from TiCl<sub>4</sub> and benzyl alcohol in the presence of 2-amino-2-(hydroxymethyl)-1,3-propanediol (HOCH<sub>2</sub>)<sub>3</sub>CNH<sub>2</sub> (Trizma).<sup>13</sup> Upon redispersion of the Trizma-functionalized titania nanoparticles in water, pearl-necklace-like structures, 4–8 nm in diameter and up to 1 μm in length, are formed (Fig. 3a). It is a notable feature that these nanowire-like arrangements are composed of a continuous string of precisely ordered nanoparticles. HRTEM investigations gave evidence that the nanoparticles assemble along the [001] direction *via* oriented attachment, exhibiting monocrystal-like lattice fringes (Fig. 3b).

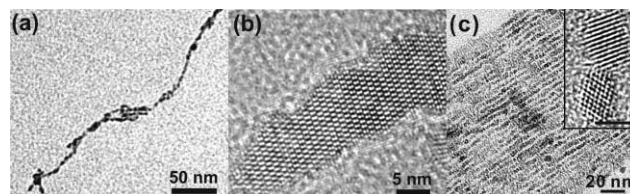


**Fig. 3** a) TEM image of wire-like titania nanoparticle assemblies, b) HRTEM of a part of such a nanostructure, c) TEM image of a comparable process of nanoparticle assembly during the crystallization of indium tin oxide (ITO) nanoparticles (inset: HRTEM of two adjacent nanoparticles, scale bar = 2.5 nm). Images a), b) and c) reprinted with permission from M. Niederberger and G. Garnweitner, *Chem.-Eur. J.*, 2006, **12**, 7282–7302 and J. Ba, A. Feldhoff, D. F. Rohling, M. Wark, M. Antonietti and M. Niederberger, *Small*, 2007, **3**, 310–317, respectively. © 2006 and 2007 Wiley-VCH.



Experimental data suggested that the anisotropic assembly is a consequence of the water-promoted desorption of the organic ligands selectively from the {001} faces of the crystalline nanosized building blocks together with the dissociative adsorption of water on these crystal faces. Both processes induce the preferred attachment of the titania nanoparticles along the [001] direction.<sup>14</sup> Such oriented attachment of titania nanoparticles was observed under hydrothermal conditions (to our knowledge, the first papers are ref. 15 and 16); the use of ligands, however, improves the perfection and extent of this alignment process.

Ordered nanoparticle assemblies were also observed during the crystallization process of indium tin oxide nanoparticles (Fig. 3c).<sup>17</sup> Although the 4 nm sized nanoparticles are almost perfectly aligned into striated two-dimensional arrays, the lattice fringes of the individual nanobuilding blocks are not oriented with respect to each other (Fig. 3c, inset). Obviously, the anisotropic interactions in ITO are only weakly related to the crystal orientation and speculatively related to the mobile electron plasma within those conducting particles. Regarding future work on the controlled assembly of nanoparticles into complex structures it is important to determine how these nanoparticles can align to form extended arrays without any mutual orientation of the crystal lattices.

The controlled desorption of ligands to align nanoparticles into nanowires is meanwhile carried out in a variety of ways, using for instance Mn-doped PbSe-nanoparticles which show remarkably nice stacking behaviour (Fig. 4).<sup>18</sup> Other examples of 1d-oriented attachment include the synthesis of ZnO nanorods,<sup>19</sup> and MnO multipods.<sup>20</sup> A recent review by Tang and Kotov also discusses other cases of one dimensional assembly of nanoparticles.<sup>21</sup>

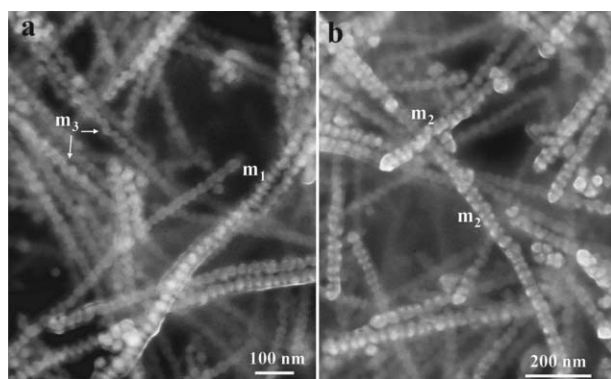


**Fig. 4** Morphologies and structural characteristics of  $\text{Pb}_{0.996}\text{Mn}_{0.004}\text{Se}$  corrugated nanoarrays after 5 min of growth. (a and b) SEM micrographs, indicating that these zigzag corrugated nanoarrays were self-assembled by uniform-sized nanoparticles according to specific stacking modes. HRTEM images (not shown) indicate that well-defined crystallographic planes are maintained over many particles. Reprinted with permission from W. G. Lu, P. X. Gao, W. Bin Jian, Z. L. Wang and J. Y. Fang, *J. Am. Chem. Soc.*, 2004, **126**, 14816–14821. © 2004 American Chemical Society.

We wish to underline that the cases given above are more defined versions or clearer model cases of a general phenomenon described in previous literature as “oriented attachment”.<sup>16</sup> More cases of “oriented attachment” are collected in ref. 32 which is a review which focuses on outer organization forces rather than particle inherent interactions. The cases discussed in this Perspective can indeed—due to the simplicity of the solvent systems—exclude the

presence of outer forces *i.e.* we regard the observed phenomena as clear cases of “self-organization”.

## Self-orientation effects while generating mesoporous films by EISA (“soft lithography”)

Another very current topic of chemistry is the fabrication of crack-free metal oxide coatings, both dense or with well-defined mesoporosity, where the structure consists of crystalline nanoparticles. Such films are considered to have advantageous properties given by the crystalline oxides (hardness, conductance, catalytic activity, sensing, redox behaviour), while accessible porosity or surface area can enhance the characteristic property of the respective oxide. Since top-down approaches failed to provide a general tool to create well-defined porosity on the nanometer-scale in metal oxide films, “evaporation-induced self-assembly” (EISA) offers an elegant and feasible pathway. EISA was first introduced by Brinker *et al.*,<sup>22</sup> but is derived from the “true nanocasting” approach,<sup>23</sup> in which lyotropic mesophases of surfactants are converted into their inorganic replicas through sol-gel templating.

In EISA, one starts from a homogeneous solution of the metal oxide precursor and templates with a significant amount of volatile solvents with low viscosity. Standard coating techniques, *i.e.* dip-coating, spin-coating, doctor-blading, or spraying allow generation of coatings with excellent macroscopic homogeneity. Evaporation of the volatile solvent produces a high concentration oxide-template phase, which is then trapped as a glassy film. The crystallinity within the pore walls is achieved by suitable post-treatment of the films at elevated temperatures.<sup>24</sup> The preparation of crack-free, homogeneous metal oxide films with high crystallinity and well-defined mesoporosity was improved by the rational choice of more suitable block copolymers, (poly(ethylene-*co*-butylene)-*b*-poly(ethylene oxide) (“KLE-polymers”)<sup>25</sup> and poly(isobutylene)-*b*-poly(ethylene oxide) (PIB-*b*-PEO).<sup>26</sup> Using such advanced templates, practically every metal oxide can be prepared in the form of thin films with highly ordered mesostructures and a high degree of crystallinity between the pore walls (Fig. 5), *e.g.*  $\text{WO}_3$ ,<sup>27</sup>  $\text{TiO}_2$ ,<sup>28</sup> and  $\text{SnO}_2$ .<sup>29</sup> A straightforward dip-coating procedure, for instance, leads to films with very good homogeneity and extremely low surface roughness (<1 nm, Fig. 5d), and even ultra thin-mesoporous films down to a single layer of micelles can be made (Fig. 5e).

For EISA in thin films, the strong interaction with the substrate in combination with a directional drying pressure (*e.g.* in dip coating) usually leads to a high degree of preferred orientation of the mesostructure, much higher as compared to bulk materials. These interactions result in a high orientation of the mesostructure (*e.g.* for cubic structures the [111] plane of FCC is usually exposed),<sup>30</sup> but under appropriately chosen conditions, the forming nanocrystals also become iso-oriented with respect to their lattice planes. As many material properties are tensorial (*e.g.* conductivity, piezo-electricity) and are deteriorated by nanoparticle grain boundaries, the advantages of controlling such an oriented self-process become immediately obvious.

A recent publication<sup>31</sup> elaborated the conditions under which straightforward EISA processing allowed the generation of both mesoporous and dense films with iso-oriented nanocrystals. The technique works especially well for certain metal oxides with

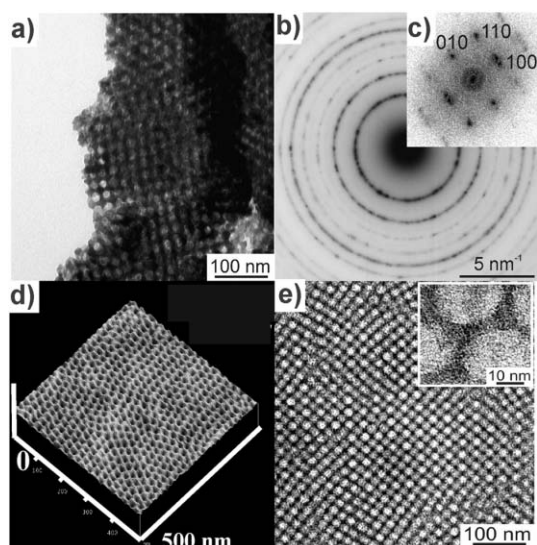


**Fig. 5** a) TEM image of mesoporous, crystalline  $\text{WO}_3$ , and b) selected area electron diffraction pattern of the same area. c) Power spectrum: Fourier transform of an area of  $23 \times 23$  nm revealing characteristic reflections of monoclinic  $\text{WO}_3$  (JCPDS: 43-1035). d) Atomic force microscopy image of a  $\text{WO}_3$  film. e) TEM and HRTEM (inset) images of a monolayer of ordered spherical mesopores ( $\text{TiO}_2$ ).

high structural anisotropy, *e.g.*  $\text{MoO}_3$ ,  $\text{Ta}_2\text{O}_5$ ,  $\text{Nb}_2\text{O}_5$  and  $\text{V}_2\text{O}_5$ , both as porous (Fig. 6b) and dense films, and also depends on having a critical amount of the correct surfactant. Both electron diffraction (Fig. 6c) as well as wide-angle X-ray scattering (Fig. 6e) shows patterns indeed indicative of a uniform crystallographic alignment of the nanocrystals. This is particularly remarkable for the mesoporous films (Fig. 6b,c), because the crystals undergo an iso-oriented nucleation and growth within the confinement of the pore walls (Fig. 6d).

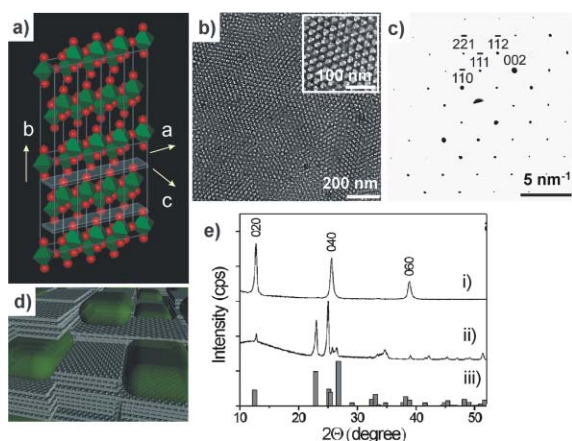


**Fig. 6** a) Illustration of the unit cells of  $\text{MoO}_3$  (molybdate). b) TEM image of a  $\text{MoO}_3$  film (treated at  $450^\circ\text{C}$ , the inset is a magnified image) and c) the SAED pattern of the same zone (*ca.*  $1\ \mu\text{m}$  times;  $1\ \mu\text{m}$ ). d) High resolution electron microscopy indicating the perfect crystallographic register of nanoparticles around a pore. e) 1D XRD patterns of a mesoporous  $\text{MoO}_3$  film indicating complete orientation (i), a film prepared without surfactant with all peaks (ii), and from the JCPDS database (iii).

This surprising finding was attributed to the special unit cell characteristics of these oxides. For instance, the peculiar atomic structure of molybdate (Fig. 6a) can be regarded as rows of  $\text{MoO}_6$  octahedra, resulting in alternating oxygen-rich and molybdenum-rich sheets perpendicular to the long *b*-axis (here the axis of orientation). These planes lead to a higher electronic polarizability in the atomic layers perpendicular to the  $[010]$  direction. The resulting self-organization towards crystallographically oriented mosaics is then quite easily explained. The orientation of the crystals with maximal polarizability parallel to the surface is the orientation of maximum attraction, as well as this, parallel polarizability tensors are also optimal for the mutual particle–particle interaction. This is very similar to the mechanism by which nanoparticles align in solution. In other words, the observation that the nanocrystals align with respect to the substrate, and also with respect to each other can be traced back to the fact that the mutual interactions of objects with a directional van der Waals force are maximal for iso-oriented arrays.

As this alignment does not depend on the material of the surface (gold, glass, Si-wafer) and especially not on a regular, fitting surface structure, as is required for epitaxy, we named the process “soft epitaxy”. The role of the surfactant is to balance the different interfacial energies of the surface and the oxide film. Furthermore, an increased surface mobility by surfactant lubrication is certainly beneficial. Another point to be mentioned for potential applications is that this mechanism always results in an orientation where the maximal conductivity is within the plane while the piezoelectric vector is perpendicular to it. This is usually also the preferred orientation of the material.

### Polymer controlled crystallization: highly parallel nanocrystallization and mesocrystal formation

The third class of experiments where spontaneous nanoparticle alignment is observed is presumably the most general one, namely additive controlled crystallization of minerals. Throughout many observations of indeed hundreds of groups (for two reviews, see ref. 32,33), it turned out that crystallization does not only progress along the textbook view, *i.e.* by nucleation and growth *via* addition of single molecules or ions, but can also express a pronounced nanoparticle phase. This is especially true for very high supersaturations or low absolute solubilities of the material to be crystallized, and when the intermediate states are stabilized against aggregation and rapid growth, for instance by polymer additives.

Then, in a highly parallel process, molecular super-saturation is lowered by first forming liquid or amorphous nanoparticle intermediates, which can then form nanocrystals as the primary species of relevance. For sufficiently high nanoparticle concentrations (which can be still as low as  $1\ \text{g L}^{-1}$ ), these nanoparticles interact and organize, taking interactions which are sufficiently anisotropic to discriminate different directions for granted.

The employment of nanobuilding block construction is essentially bioinspired, as nature uses the same principles to construct biominerals. The idea to mimic these multi-building block principles for the construction of modern organic–inorganic hybrid materials was recently well summarized in two review articles.<sup>34,35</sup>

A particularly nice case is the crystallization of  $\text{BaSO}_4$ , where a multiplicity of extraordinary shapes can be realized (*e.g.* see ref. 36–40). This is due to the low solubility of barite, together



with the high anisotropy of its unit cell. Such a structure which can extend over millimeters in three directions is shown in Fig. 7.

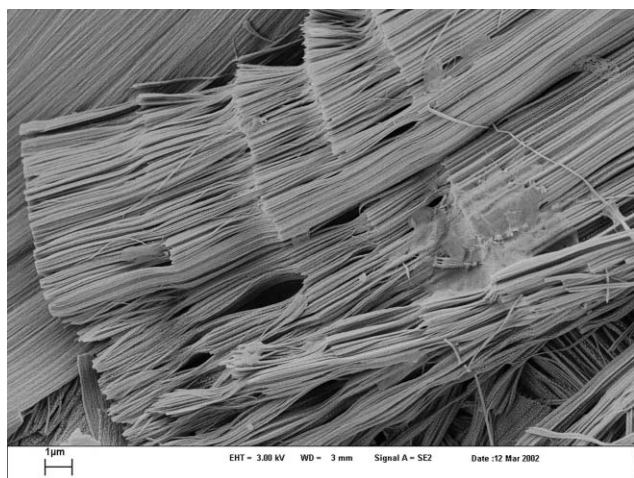


**Fig. 7** Complex forms of  $\text{BaSO}_4$  fiber bundles produced in the presence of 0.11 mM sodium polyacrylate ( $M_n = 5100$ ), at room temperature,  $[\text{BaSO}_4] = 2 \text{ mM}$ ,  $\text{pH} = 5.5$ , 4 d crystallization time. Reprinted with permission from H. Cölfen and S. H. Yu, *MRS Bull.*, 2005, **30**, 727–735.<sup>41</sup> © 2005 Materials Research Society.

Obviously the primary  $\text{BaSO}_4$  nanoparticles (*ca.* 20–50 nm size) first align and crystallize to form extended one-dimensional fibers, which (presumably by parallel crystallization) form extended bundles with smectic type splitting planes. The observed morphology is, in this case, a 100% event, *i.e.* all the  $\text{BaSO}_4$  crystallizes in this way.

The scattering of such a structure is practically that of a single crystal, except that a slight angular broadening caused by the bends and defects is already visible in the SEM picture. This makes it obvious that the controlled nanoparticle alignment can go over all three dimensions and in a hierarchical fashion over millimeters, keeping a common orientation of the superstructure. Due to spontaneous structure formation on the mesoscale by a self-organization process and the many similarities to the formation of mesophases in liquid crystals, these structures were named “mesocrystals”.<sup>33,42</sup>

Knowing the appropriate parameter window, this “parallel” crystallization to nanoparticles and alignment to a superstructure can even be induced in the most ordinary crystallization systems, such as for  $\text{CaCO}_3$ . The presence of small amounts of simple polyelectrolytes, such as polystyrenesulfonate (PSS), allows “morphing” of the calcite crystal,<sup>43</sup> as depicted and explained in Fig. 8.

The resulting structures are stable to recrystallization, exhibit curved outer shapes, roughness and porosity, but are nevertheless almost perfect in their vectorial alignment. A conservative estimate based on kinetic observations indicates that at least  $10^9$  primary nanoparticles have aligned *via* “mesocrystallization” to form such three-dimensional hierarchical superstructures, strictly following, however, a “program” encoded in the primary reaction condition and the added polymer. Furthermore it is interesting to observe that mistakes mainly occur on the mesoscale, but obviously “grow out” at the larger scale as order clearly goes through a minimum. This means that such self-organization is obviously error-tolerant.

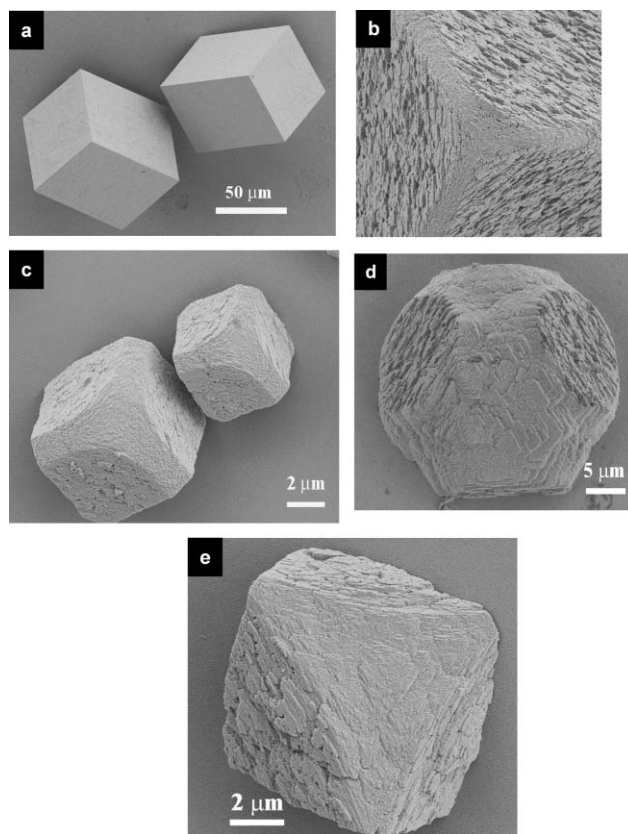


**Fig. 8** “Morphing series” of Calcite/ $\text{CaCO}_3$  by crystallization in the presence of different amounts of PSS: a) Default reaction leading to rhombohedral calcite; b) 100 mg PSS  $\text{L}^{-1}$  reveal that the crystal is a rough “superstructure”, edges and corners are removed; c) & d) Increasing PSS concentration amplifies the effect, the second structure is a rounded crystal with 6 elliptic side faces; e) 1 g  $\text{L}^{-1}$  PSS gives a mesocrystal which is a double triangular truncated rhombohedron; f) Zooming into the structure indicates that the superstructure is indeed composed of subunits arranged in a hierarchical fashion, however, following almost perfect vectorial alignment. Pictures reprinted with permission from T. X. Wang, M. Antonietti and H. Cölfen, *Chem.–Eur. J.*, 2006, **12**, 5722–5730. © 2006 Wiley-VCH.

## Discussion and conclusion

The three selected cases discussed in this Perspective, namely, assembler-encoded nanoparticles, soft epitaxy of thin films, and polymer controlled crystallization all rely on spontaneous organization of nanoparticles towards sometimes astonishingly complex superstructures by a self-process.

It is through the synthetic procedures used that this process can be controlled: choosing appropriate solvents and reaction conditions, ligands, special functional additives or polymers, the faces of the primary nanoparticles can be “colour-coded”, adding charged or hydrophobic patches supporting the mutual alignment. Sometimes, sufficient colloidal stabilization, which allows reorientation, coupled with the inherent anisotropy of the nanoparticles is enough to induce the organized assembly process.

Calling on an allegory: inorganic nanoparticles, once appropriately stabilized, can obviously be “polymerized” towards organized structures. Contrary to organic monomers, this polymerization can be one-, two-, or three-dimensional, depending on

the interactions which can be addressed. We exemplified linear arrays of nanoparticles, by ligand exchange, two dimensional mosaic arrays in WO<sub>3</sub> plates and in soft epitaxy, while simple polymer controlled crystallization can result in quite sophisticated 3D-superstructures once the appropriate conditions are chosen. It is a supramolecular chemistry using inorganic nanocrystals as building blocks.

Humankind is attracted by symmetry and order, but even more so by complexity and emergence within such systems. In these terms, the observed patterns feel “natural” and beautiful, and it is a deep, rather humanistic question as to why this is the case.

The resulting structures are, however, not only aesthetically appealing, but obviously have potential as chemical products, *i.e.* applications in chemical and mechanical sensing, electrochromic devices, photovoltaics, as sorption materials or for molecular storage devices can be envisaged, as discussed in the single articles referenced herein.

## References

- 1 J.-M. Lehn, *Supramolecular Chemistry—Concepts and Perspectives*, VCH Verlagsgesellschaft mbH, Weinheim, 1995.
- 2 B. G. G. Lohmeijer and U. S. Schubert, *J. Polym. Sci., Part A: Polym. Chem.*, 2003, **41**, 1413–1427.
- 3 H. Li, M. Eddaoudi, M. O’Keeffe and O. M. Yaghi, *Nature*, 1999, **402**, 276–279.
- 4 G. Férey, C. Mellot-Draznieks, C. Serre, F. Millange, J. Dutour, S. Surble and I. Margiolaki, *Science*, 2005, **309**, 2040–2042.
- 5 M. Antonietti and C. Göltner, *Angew. Chem., Int. Ed. Engl.*, 1997, **36**, 910–928.
- 6 M. Niederberger and G. Garnweitner, *Chem.–Eur. J.*, 2006, **12**, 7282–7302.
- 7 G. Garnweitner and M. Niederberger, *J. Am. Ceram. Soc.*, 2006, **89**, 1801–1808.
- 8 M. Niederberger, M. H. Bartl and G. D. Stucky, *J. Am. Chem. Soc.*, 2002, **124**, 13642–13643.
- 9 J. Polleux, N. Pinna, M. Antonietti and M. Niederberger, *J. Am. Chem. Soc.*, 2005, **127**, 15595–15601.
- 10 J. Polleux, M. Antonietti and M. Niederberger, *J. Mater. Chem.*, 2006, **16**, 3969–3975.
- 11 J. Polleux, A. Gurlo, N. Barsan, U. Weimar, M. Antonietti and M. Niederberger, *Angew. Chem., Int. Ed.*, 2006, **45**, 261–265.
- 12 J. Polleux, N. Pinna, M. Antonietti and M. Niederberger, *J. Am. Chem. Soc.*, 2005, **127**, 15595–15601.
- 13 J. Polleux, N. Pinna, M. Antonietti and M. Niederberger, *Adv. Mater.*, 2004, **16**, 436–439.
- 14 J. Polleux, N. Pinna, M. Antonietti, C. Hess, U. Wild, R. Schlögl and M. Niederberger, *Chem.–Eur. J.*, 2005, **11**, 3541–3551.
- 15 R. L. Penn and J. F. Banfield, *Am. Mineral.*, 1998, **83**, 1077–1082.
- 16 R. L. Penn and J. F. Banfield, *Geochim. Cosmochim. Acta*, 1999, **63**, 1549–1557.
- 17 J. Ba, A. Feldhoff, D. F. Rohling, M. Wark, M. Antonietti and M. Niederberger, *Small*, 2007, **3**, 310–317.
- 18 W. G. Lu, P. X. Gao, W. Bin Jian, Z. L. Wang and J. Y. Fang, *J. Am. Chem. Soc.*, 2004, **126**, 14816–14821.
- 19 C. Pacholski, A. Kornowski and H. Weller, *Angew. Chem., Int. Ed.*, 2002, **41**, 1188–1191.
- 20 D. Zitoun, N. Pinna, N. Frolet and C. Belin, *J. Am. Chem. Soc.*, 2005, **127**, 15034–15035.
- 21 Z. Tang and N. A. Kotov, *Adv. Mater.*, 2005, **17**, 951–962.
- 22 C. J. Brinker, *MRS Bull.*, 2004, **29**, 631–640.
- 23 G. S. Attard, J. C. Glyde and C. G. Goltner, *Nature*, 1995, **378**, 366–368.
- 24 D. Grosso, F. Cagnol, G. Soler-Illia, E. L. Crepaldi, H. Amenitsch, A. Brunet-Bruneau, A. Bourgeois and C. Sanchez, *Adv. Funct. Mater.*, 2004, **14**, 309–322.
- 25 A. Thomas, N. Schlaad, B. Smarsly and M. Antonietti, *Langmuir*, 2003, **19**, 4455–4459.
- 26 M. Groenewolt, T. Brezesinski, H. Schlaad, M. Antonietti, P. W. Groh and B. Iván, *Adv. Mater.*, 2005, **17**, 1158–1162.
- 27 T. Brezesinski, D. Fattakhova Rohlfing, S. Sallard, M. Antonietti and B. Smarsly, *Small*, 2006, **2**, 1203–1211.
- 28 B. Smarsly, D. Grosso, T. Brezesinski, N. Pinna, C. Boissière, M. Antonietti and C. Sanchez, *Chem. Mater.*, 2004, **16**, 2948–2952.
- 29 T. Brezesinski, A. Fischer, K.-I. Iimura, C. Sanchez, D. Grosso, M. Antonietti and B. Smarsly, *Adv. Funct. Mater.*, 2006, **16**, 1433–1440.
- 30 M. Kuemmel, D. Grosso, C. Boissière, B. Smarsly, T. Brezesinski, P. A. Albouy, H. Amenitsch and C. Sanchez, *Angew. Chem., Int. Ed.*, 2005, **44**, 4589–4592.
- 31 T. Brezesinski, M. Groenewolt, N. Pinna, H. Amenitsch, M. Antonietti and B. Smarsly, *Adv. Mater.*, 2006, **18**, 1827–1831.
- 32 H. Cölfen and S. Mann, *Angew. Chem., Int. Ed.*, 2003, **42**, 2350–2365.
- 33 H. Cölfen and M. Antonietti, *Angew. Chem., Int. Ed.*, 2005, **44**, 5576–5591.
- 34 C. Sanchez, G. G. Soler-Illia, F. Ribot, T. Lalot, C. R. Mayer and V. Cabuil, *Chem. Mater.*, 2001, **13**, 3061–3083.
- 35 C. Sanchez, H. Arribart and M. M. Giraud-Guille, *Nat. Mater.*, 2005, **4**, 277–288.
- 36 M. Li and S. Mann, *Langmuir*, 2000, **16**, 7088–7094.
- 37 L. Qi, H. Cölfen and M. Antonietti, *Chem. Mater.*, 2000, **12**, 2392–2403.
- 38 S.-H. Yu, H. Cölfen and M. Antonietti, *Chem.–Eur. J.*, 2002, **8**, 2937–2945.
- 39 H. Cölfen, L. M. Qi, Y. Mastai and L. Börger, *Cryst. Growth Des.*, 2002, **2**, 191–196.
- 40 M. Li, H. Cölfen and S. Mann, *J. Mater. Chem.*, 2004, **14**, 2269–2276.
- 41 H. Cölfen and S. H. Yu, *MRS Bull.*, 2005, **30**, 727–735.
- 42 T. Wang, H. Cölfen and M. Antonietti, *J. Am. Chem. Soc.*, 2005, **127**, 3246–3247.
- 43 T. X. Wang, M. Antonietti and H. Cölfen, *Chem.–Eur. J.*, 2006, **12**, 5722–5730.